3D puzzle-inspired construction of large and complex organ structures for tissue engineering

Zheng-Tian Xie [a], Jinfeng Zeng [a], Shigeru Miyagawa [b], Yoshiki Sawa [b], Michiya Matsusaki [a,*]

[a] *Division of Applied Chemistry, Graduate School of Engineering, Osaka University, 2-1 Yamadaoka, Suita, Osaka, 565-0871, Japan*
[b] *Department of Cardiovascular Surgery, Osaka University Graduate School of Medicine, 2-2 Yamadaoka, Suita, Osaka, 565-0871, Japan*

ARTICLE INFO

ABSTRACT

3D printing as a powerful technology enables the fabrication of organ structures with a programmed geometry, but it is usually difficult to produce large-size tissues due to the limited working space of the 3D printer and the instability of bath or ink materials during long printing sessions. Moreover, most printing only allows preparation with a single ink, while a real organ generally consists of multiple materials. Inspired by the 3D puzzle toy, we developed a "building block-based printing" strategy, through which the preparation of 3D tissues can be realized by assembling 3D-printed "small and simple" bio-blocks into "large and complex" bioproducts. The structures that are difficult to print by conventional 3D printing such as a picture puzzle consisting of different materials and colors, a collagen "soccer" with a hollow yet closed structure, and even a full-size human heart model are successfully prepared. The 3D puzzle-inspired preparation strategy also allows for a reasonable combination of various cells in a specified order, facilitating investigation into the interaction between different kinds of cells. This strategy opens an alternative path for preparing organ structures with multiple materials, large size and complex geometry for tissue engineering applications.

1. Introduction

3D printing as a cutting-edge manufacturing technology allows us to fabricate complex 3D structures with programmed geometry [1–4]. In particular, the embedded 3D printing has made a breakthrough in the realization of biomaterials printing by using jammed granular hydrogels as a supporting bath, which not only provides mechanical support to the extruded biomaterials but also offers a water-containing environment for cell-laden ink [5–12]. With the rapid development of 3D printing in the past decade, extensive research has been conducted into attempts to fabricate tissue models based on 3D bioprinting, such as muscle [13], brain [14], tumor [15], vessel models [16–19], and simple organ structures including cartilage [20,21], ear [22], nose, and even a small human heart [23] for medical research [24–26] and tissue engineering [27].

Despite these encouraging advances, 3D bioprinting still has difficulty in producing tissues or organs that meet the requirements for practical application [28]. The current state of this art is still confronted with the following challenges. First, it is difficult to simultaneously print multiple inks in a single printing. Human tissues usually consist of a variety of cells with distinct functions and heterogeneous distribution in tissue. However, in most cases only a single nozzle can be used in each bioprinting,

and multiple kinds of cells are homogeneously mixed in the ink solution to be printed [29]. Although some advanced printers equipped with multiple nozzles allow the printing of two or more inks, the switching of nozzles during the printing process requires a more complicated machine and special printing path design [30], leading to longer printing times and a high error rate in the printing process. Moreover, the printing of different inks always accompanies a change of bath condition, which also hinders the printing of a whole structure with multiple components in a single printing process. Second, current 3D bioprinting usually produces samples of a small size, and the printing of full-size large organs is still a challenge [31]. One of the reasons is the limited working space of the printer. Most commercial 3D bioprinters have a working space of only several centimeters, while some organs such as the human heart are greater than 10 cm in height. Another possible reason is related to the stability of the bath and ink materials. Even if the full-size printing of large samples can be realized by using a modified or homemade printer with an enlarged working space [32], it generally requires a longer printing time, which may cause property changes in the ink or bath [33]. For example, some granular gel baths such as thermo-sensitive gelatin and ionic-crosslinked alginate microgels in the bath may gradually aggregate with each other [34], leading to failure of the printing. When

---

cell-laden ink is used, cell death during the long printing duration is also a problem. As a result, many organ models prepared in the laboratory are always scaled down in size for easy printing [35]. Third, the bath materials encapsulated in the closed samples are difficult to remove after printing. In general, the removal of attached bath materials is mainly based on methods such as mechanical removal, thermally melting the bath (as in a gelatin bath), and the dissolution of bath gels (like GG and alginate gels). However, the bath materials that are closed in the hollow structure cannot be washed out without breaking the structure. All these abovementioned limitations in current 3D bioprinting hinder its practical application in medical research and tissue engineering.

The 3D puzzle toy provides inspiration to overcome these limitations. 3D puzzle is a well-known toy based on the strategy of assembling various small blocks to build large, complex structures. Each 3D puzzle block is a modular design and is produced in a flow-line process, while many grand and complex structures can be built using these small and simple blocks. This prompted us to consider whether we can introduce the 3D puzzle strategy into the biomedical field for tissue engineering. Like 3D puzzle toy, we may prepare a complex biostructure piece by piece. Theoretically, a target 3D model can be reasonably divided into various small and simple parts that can then be printed out one by one on a common 3D printer. After printing, each piece can be used as a bio-block to build complex tissues. By such a simple strategy, we may overcome the limitations mentioned above and achieve the following advantageous results. First, the separate preparation of different parts allows us to produce samples with varied ink components or cells in diverse printing conditions. It also enables the specific modification of each part of the final product. Second, the building block strategy makes easy the fabrication of large and complex biostructures, even on a small commercial printer. Third, the undesirable bath materials that remain on the printed bio-block can be easily removed before the blocks are assembled into a complex structure. Finally, it makes possible the modular design and flow-line production of 3D complex tissues on a large scale.

Some previous studies have reported the connection of printed samples to building complex structures. For example, Gao et al. [36] used a commercial medical glue to connect hollow vessels with different diameters to fabricate a branched vessel system. Besides this research, some similar works also mentioned the connection of printed parts to fabricate certain structures such as vessels and organoids. However, most works only focus on a certain specific application [37], few studies extend and refine the assembly method to be a more general and scalable strategy for bio-applications. In 2020, Bertassoni et al. [38] developed a building block strategy for tissue engineering using printed modular microcages as instructive scaffolds. The microcages played the role of the rigid framework with a fixed shape that can interlock with each other like LEGO toy (LEGO is a trademark of The Lego Group). The microcages have an average compressive strength of 59.2 MPa. They can be applied in bone regeneration as the mechanical strength of the microcage closely approximates that of mandibular bone, which was reported to be 56 ± 29.6 MPa. However, with such rigid blocks, it is difficult to construct soft and resilient structures. For example, human organs such as the heart and kidney have a modulus in the range of 1–100 kPa [39], which is much lower than that of the β-tricalcium phosphate ceramic or methacrylate-based resin. Moreover, the rigid sample after assembly is difficult to biodegrade when used *in vivo*. Therefore, developing an accessible 3D building-block fabrication strategy for building soft biostructures from 3D-printed blocks and systematically investigating its potential applications in tissue engineering is still necessary.

Herein, a 3D puzzle-inspired 3D printing strategy was developed to construct complex or large tissues on a small 3D printer. Small bio-blocks were separately printed on the 3D printer and then a mixture of fibrinogen and thrombin was used as a bio-glue to connect the printed bio-blocks to construct the target product. As a proof of concept, the complex structures including a picture puzzle consisting of different kinds of materials, a hollow but closed collagen "soccer", and even a full-size

collagen 3D heart model were successfully prepared by the assembly of a series of small bio-blocks. All of these are difficult to directly prepare in common 3D printing. Moreover, the 3D puzzle-inspired method enables us to specifically prepare different cell blocks and reasonably connect them, which is conducive to understanding the interaction between different cells due to the flexible structure collocation and easy observation of cell behavior. This work describes a simple and efficient 3D printing strategy to construct complex and large bio-tissues, opening an alternative route to building complex tissue or organ models for medical research and application.

2. Results and discussion

A 3D puzzle-inspired strategy was employed here to fabricate large and complex biostructures on a commercial 3D printer. As shown in Fig. 1, to construct a full-size human heart model, the different parts of the model can be individually printed and then assembled to form the final product, just like playing with 3D puzzle toy. Compared with conventional 3D printing, the 3D puzzle-inspired strategy has several advantages. First, it makes the flow-line production of 3D tissue possible. Second, it makes large-size samples possible. Third, multiple inks or cells can be used for assembly and, finally, it allows us to locally modify any part of the products before assembly.

To assemble the printed bio-pieces, a "bio-glue" that can effectively bind different bio-pieces together is necessary. Theoretically, all adhesive methods for connecting printed parts can be used for assembly. Considering the biocompatibility and easy accessibility, here the mixture of fibrinogen and thrombin is adopted as "bio-glue". It is extensively used in tissue engineering and its gelation mechanism is well established. As shown in Fig. S1, the fibrinogen will be activated under the enzyme catalysis of thrombin and then crosslinked with each other to form fibrin gel. This reaction is well known in blood coagulation in the human body. Moreover, the gelation speed as well as the fibrin gel strength can be easily monitored by changing the fibrinogen concentration in solution. Therefore, this reaction was used here to combine the printed bio-blocks. Fig. 2 (a) depicts a typical connection process of two printed collagen sheets. After putting the pairs of sheets together, the bio-glue was added into the joint gap and the two sheets were then held together for 5 min at room temperature. During this process, the flowable mixture solidified and the two collagen pieces were successfully connected. To confirm the connection effect, the fibrin gel was visualized by fluorescence-labeled fibrinogen in the bio-glue. The assembled sample was washed with PBS to remove the unreacted bio-glue, and then observed under confocal laser scanning microscope (CLSM). Fig. 2 (b) shows a CLSM image at the joint part of the sample, in which the green fluorescence signal can be seen at the binding boundary. SEM image of the connected collagen sheet also showed the fibrin gel filled in the crevice between two collagen sheets. It can be found that the collagen pieces were connected by touching each other with the bonding of fibrin gel, but not overlapping of two collagen planes (Fig. S2). All these indicate that the fibrin gel was successfully formed between the two sample pieces, which contributes to the adhesion effect. It should be noted that the binding strength, the maximum stress that the binding joint can withstand before the connection breaks, can be adjusted by changing the fibrinogen concentration in the bio-glue. As shown in Fig. 2 (c-e), the binding strength can be improved by increasing the fibrinogen concentration from 2 kPa of 20 mg/mL to 6 kPa of 100 mg/mL. However, when the fibrinogen concentration in the glue is too high (100 mg/mL), the gelation speed of the glue is too fast, and the mixed glue usually solidifies before we splice two blocks well. Therefore, the concentration of 50 mg/mL was used in the following experiments except where stated otherwise. At this concentration, the glue also exhibits good adhesion ability to prevent the break of the connection in our following experiments.

In 3D puzzle games, the assembled products can be disassociated to separate 3D puzzle blocks that can be reused to build other 3D puzzle constructs. Likewise, the assembled sample in our experiment can also be
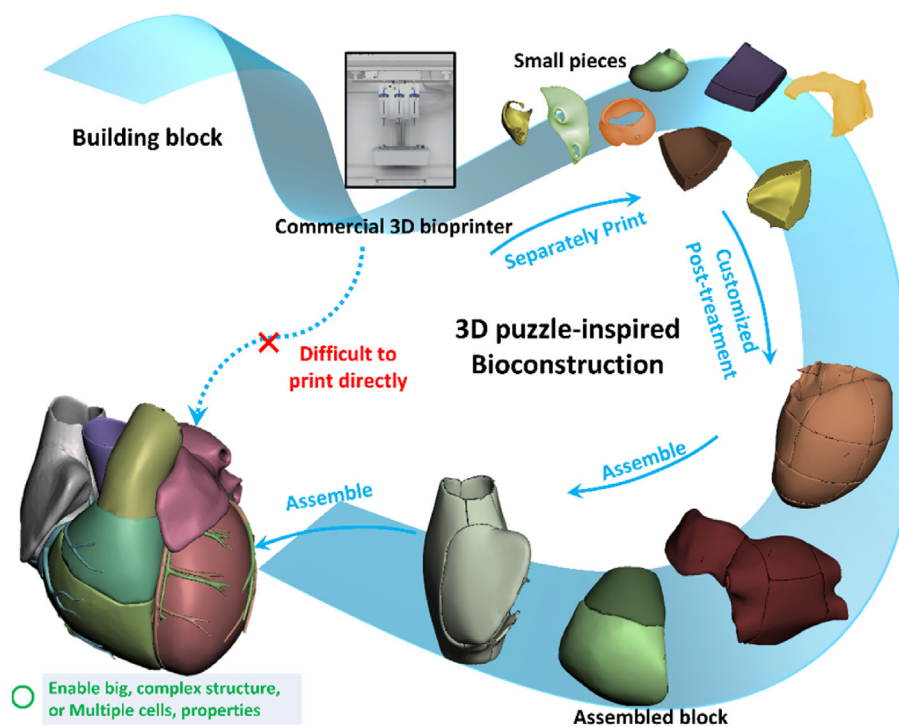
Fig. 1. Schematic diagram of the 3D puzzle-inspired printing. Complex organ structure such as an heart model can be constructed by a commercial bio-printer based on the strategy consisting of printing, customized post-treatment and assembling process.

disassociated by a simple trypsin treatment. As depicted in Fig. 2 (f), two pieces of collagen sheet connected by bio-glue were immersed in a trypsin solution in a 6-well plate and incubated at 37 °C for 10 min. During this process, the bio glue, i.e., fibrin gel, is digested by trypsin through the cleavage of lysine and arginine sites in the fibrin gel (Fig. 2 (g)). As a result, the sample was disconnected into two isolated pieces, and the disconnected pieces can be reused in another construction. Fig. S3 showed CLSM images of the boundary region during the disassociation process. It was found that the fluorescence intensity gradually increased after immersing in the trypsin solution, indicating that the fluorescence-labeled fibrin gel was digested and leaked out from the joint.

In conventional 3D printing, the production of a structure with multiple components requires the switching of inks in the printing process, which requires machines equipped with multiple nozzles and the specific design of printing path. This is usually time-consuming and has a high error rate. The strategy developed in this work removes this limitation. Since each component can be separately printed as a block to build a complex structure, this strategy makes the standardized and scaled production of the complex structure on a commercial printer possible. As shown in Fig. 3 (a), the OMA squares with black staining and the collagen squares with a white color are separately printed as blocks to construct the desired patterns (Fig. 3 (b)). As illustrated in Fig. 3 (c and d), a picture puzzle with a size of 11 cm × 6 cm was successfully fabricated by assembling a total of 66 pieces of the printed OMA and collagen blocks. In detail, the fibrinogen and thrombin in PBS were mixed in a 1.5 mL centrifugation tube by pipette and then immediately added into the seam between two sheets. After keeping at room temperature for several minutes, the fibrinogen will react with thrombin to form fibrin gel, by which two pieces of blocks can be connected. Since the connection process was conducted on the glass plate, the connected sheets are basically kept in the same plane, as shown in Fig. 3c. In this puzzle, the letters "O" and "U" were assembled with the black OMA squares, while the white collagen squares were connected as the background. The obtained picture puzzle can be picked up by hand without it falling apart, demonstrating the connective efficacy of the bio-glue. The 3D puzzle-

inspired strategy also allows us to print some special 3D shapes that are difficult to prepare in common 3D printing. For example, a structure with a hollow yet closed spherical shell shape is hard to prepare in a single 3D printing, because the soft and watery biomaterials usually require a supporting bath (such as fluidic granular gels) during the printing process to avoid collapse due to gravity. In this case, the bath materials remaining inside the closed shell cannot be removed without breaking the sample once the printing is finished. Our 3D puzzle-inspired printing can solve this problem. As shown in Fig. 3 (e-j), the collagen hexagon and pentagon were separately printed with 1 wt% and 2 wt% collagen ink in a GG microgel bath that contained 0.3 M trisodium citrate (TSC) or 30 v/v% ethanol, respectively. After releasing from the bath and post-treatment by washing and crosslinking, they were assembled to build a hollow and closed truncated icosahedron, a "collagen soccer", also known as the structure of fullerene (C_{60}). Since each part of the spherical shell is prepared individually and has a very simple geometry, the attached bath materials can be easily washed out before the assembly into the final closed product.

The 3D puzzle-inspired strategy also enables 3D printing construction of biostructures with a large size. Although 3D printers for thermoplastic materials or inorganic concrete are already capable of printing large sizes in the meter scale [40], the current state of printing for biomaterials usually produces samples with sizes below 5 cm [41–43]. This is probably because 3D printing for tissue engineering and organ fabrication is still in the experimental stage and most commercial 3D printers have a small working space. More importantly, the printing of soft biomaterials requires supporting bath materials to provide the water environment, but the long printing duration for a big sample may lead to changes in the bath and ink during the printing process. The developed method in this work removes these shackles and allows us to prepare big organ structures even on a printer in laboratory. To demonstrate this, a full-size human heart model was prepared using our printing and assembly strategy. The heart is one of the most complex organs in the human body and many attempts have been made to fabricate a model of it *in vitro* by 3D printing [23,35]. However, most prepared heart models in the literature have a small size with a diameter below 5 cm. Only one study has
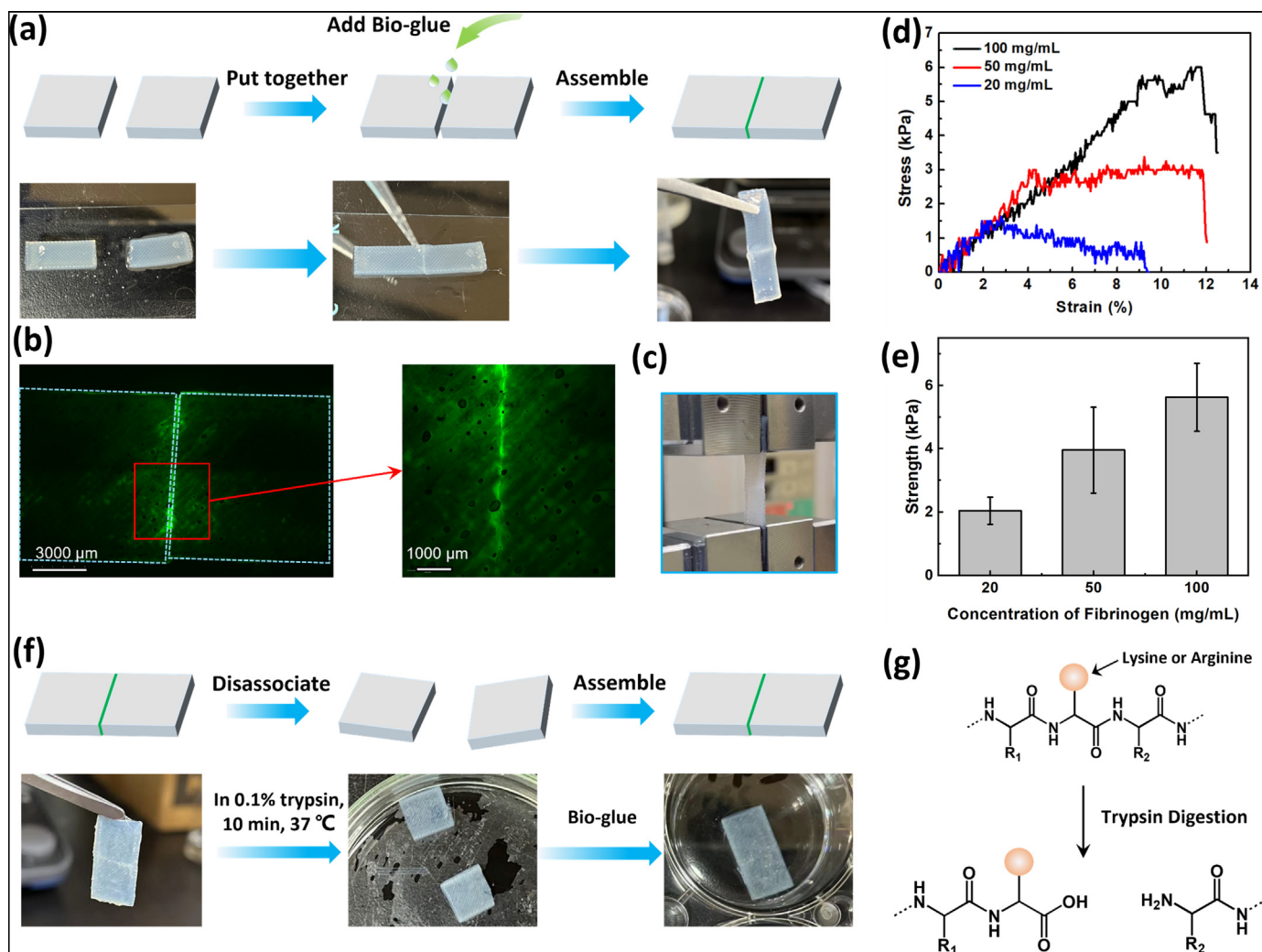
Fig. 2. Assembly and disassembly process of the printed collagen blocks. **(a)** Assembly process of two pieces using the mixture of fibrinogen and thrombin as a "bioglue" **(b)** Fluorescence images of the jointed area of the assembled sample. **(c)** Digital photo of the sample during the mechanical test. **(d)** Strain-stress curve of the samples connected by bio-glue with different fibrinogen concentrations and **(e)** the break strength calculated from the strain-stress curves. **(f)** Disassociation and reconnection of the pieces using trypsin digestion. **(g)** Mechanism of the trypsin digestion.

attempted to prepare a full-size heart by 3D printing of alginate on their own homemade printer [32]. In our experiment, the full-size heart was 3D printed piece by piece on a commercial 3D printer. Fig. 4 (a) shows a 3D digital model of the human heart. It consists of four chambers, i.e., left atrium, right atrium, left ventricle, and right ventricle, as shown in Fig. 4 (b). To realize the printing of a full-size heart, the whole model was further split into a total of more than 60 small pieces (Fig. S4). Each small piece had a size of less than 5 cm, which could be easily printed on a common 3D printer, as demonstrated in Fig. S5 and Fig. 4 (c). Similarly, the blood vessels of the heart could also be printed segmentally (Fig. 4 (d)). As shown in Fig. S6, the printed product was crosslinked and then released from the bath. Fig. 4 (e) shows the printed collagen pieces after crosslinking and washing. These collagen blocks were further assembled to construct the heart model. As shown in Fig. 4 (f and g), the left atrium, right atrium, left ventricle, and right ventricle were firstly prepared, and then connected to each other. Finally, a full-size collagen heart was successfully constructed (Fig. 4 (h) and Fig. S7). Since the 3D puzzle-inspired method produces big samples based on a "gather the small into big" process, a big organ can be constructed even on a small printer. Moreover, the modular production of the small blocks of a big organ allows us to specifically design and replace certain pieces on the organ without changing the other parts, which is conducive to the targeted investigation of parts that are of particular interest in a big organ.

Human tissues usually consist of multiple cells with distinct functions. Although some advanced printers enable the printing of two or three bioinks by using multiple switchable nozzles, it is still difficult to fabricate a whole tissue by a single 3D printing, as different kinds of cells may require different bath environments and culture conditions. The 3D puzzle-inspired strategy allows us to construct tissues with different cells through a "printing, culture and assembly" process. The bio-blocks with various cells can be separately prepared then used to build the desired bioproducts by the reasonable connection of these bio-blocks. The modular design and preparation process not only removes the limitation of most commercial printers that only support one kind of ink, but also makes it easy to study the interaction between different cells. As a proof of concept, the effect of NHDF on the capillarization of HUVEC was investigated by assembling these two kinds of cells according to certain patterns. For the visualization of the cell location, red fluorescence-labeled NHDF (RF-NHDF) and GFP-HUVEC were used in this experiment. As illustrated in Fig. 5 (a), the RF-NHDF and GFP-HUVEC with a cell density of 1×10^6 cells/cm^2 were seeded on a printed collagen sheet. After culture for 1 day in KBM or DMEM medium respectively, the obtained collagen sheets were used as blocks to construct a 3×3 square, in which the GFP-HUVEC block was in the center and the RF-NHDF blocks were located at the left and right side of the HUVEC piece. As a control, collagen blocks at other region bear no cells. CLSM images of the sample
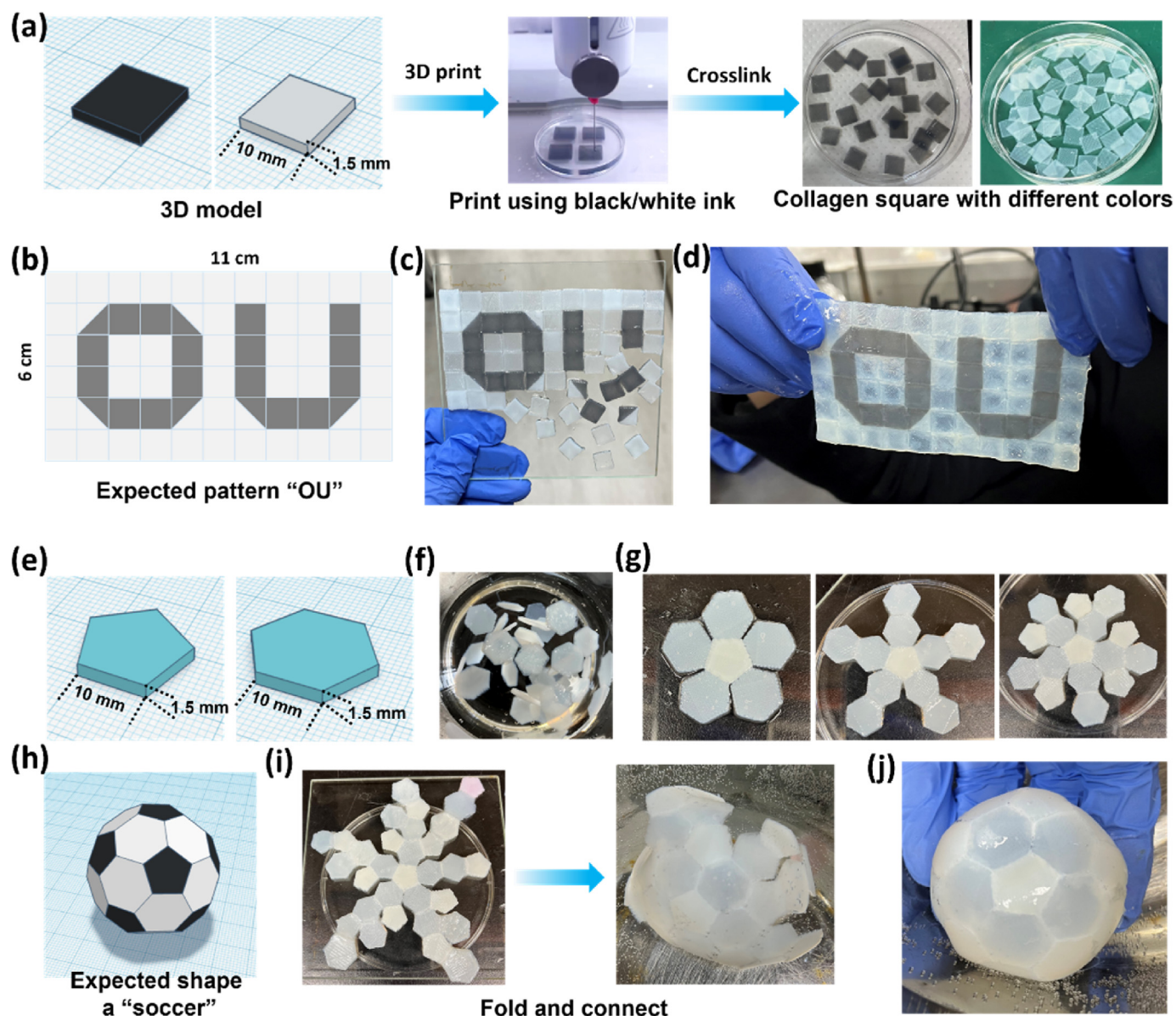
Fig. 3. Fabrication of complex structures by 3D puzzle-inspired assembly of 3D printed pieces. **(a)** Preparation process of the white/black pieces with a square shape by 3D printing. **(b)** a designed pattern with "O U" characters. **(c)** The assembling process using the white/black pieces. **(d)** Assembled product with the designed patterns. **(e)** Designed 3D models with the pentagon and hexagon shape. **(f)** The pentagon and hexagon obtained by 3D printing using 2 wt% and 1 wt% collagen ink. **(g)** Connection of the pieces with pentagon and hexagon shape. **(h)** Designed 3D models with a soccer shape. **(i)** preparation process of the hollow soccer shape by folding and connecting the pieces. **(j)** Assembled collagen product with the designed hollow soccer shape.

after assembly are presented in Fig. 5 (b) and show clear boundaries between the GFP-HUVEC region (green) and the RF-NHDF region (red). After continuous culturing of the assembled sample for 4 days, capillary formation could be found at the boundary between the two kinds of cells. As illustrated in Fig. 5 (c), the capillaries sprout from the edge of the GFP-HUVEC blocks and grow into the NHDF blocks. When cultured for a longer time (e.g., 10 days), the capillaries became longer, and more newly formed capillaries could be found. Thus, it can be interpreted that the NHDF can induce capillary formation of HUVEC by secreting specific growth factors. Fig. 5 (c) shows that the capillaries mainly appeared at the boundary with NHDF, but were hard to find at the boundary without NHDF cells. To clearly observe the capillaries, another sample after culturing for 10 days under the same conditions was fixed, and the specific protein CD31 of HUVEC was immunostained. As a result, capillaries with a dendritic structure could be clearly observed. Moreover, the capillaries mainly grew towards the NHDF side, but not randomly grew

on both sides, as shown in Fig. 5 (d). Besides the capillary formation, the effect of NHDF on the migration of HUVEC can also be investigated by this assembled model. From Fig. 5 (c), we can observe that HUVEC tends to migrate to the area without cells (up and down direction) rather than the area that is occupied by NHDF (left and right direction). This may be caused by the fact that the area without cells has more nutrients and oxygen. Compared with studies that are based on the homogeneous mixture and NHDF and HUVEC, the 3D puzzle-inspired assembly provided a simple approach to flexibly designing and connecting the NHDF and HUVEC blocks. The versatile collocation of NHDF and HUVEC and easy observation of the cell behavior such as the migration and capillary extension direction make this technique conducive to understanding the interaction between them. Although it is still far away from the replication of the function of a real tissue as the natural organ is a complex system that involves multiple cells behaviors, various mass transferring and bioreactions, the "print, culture and assembly" method provided an
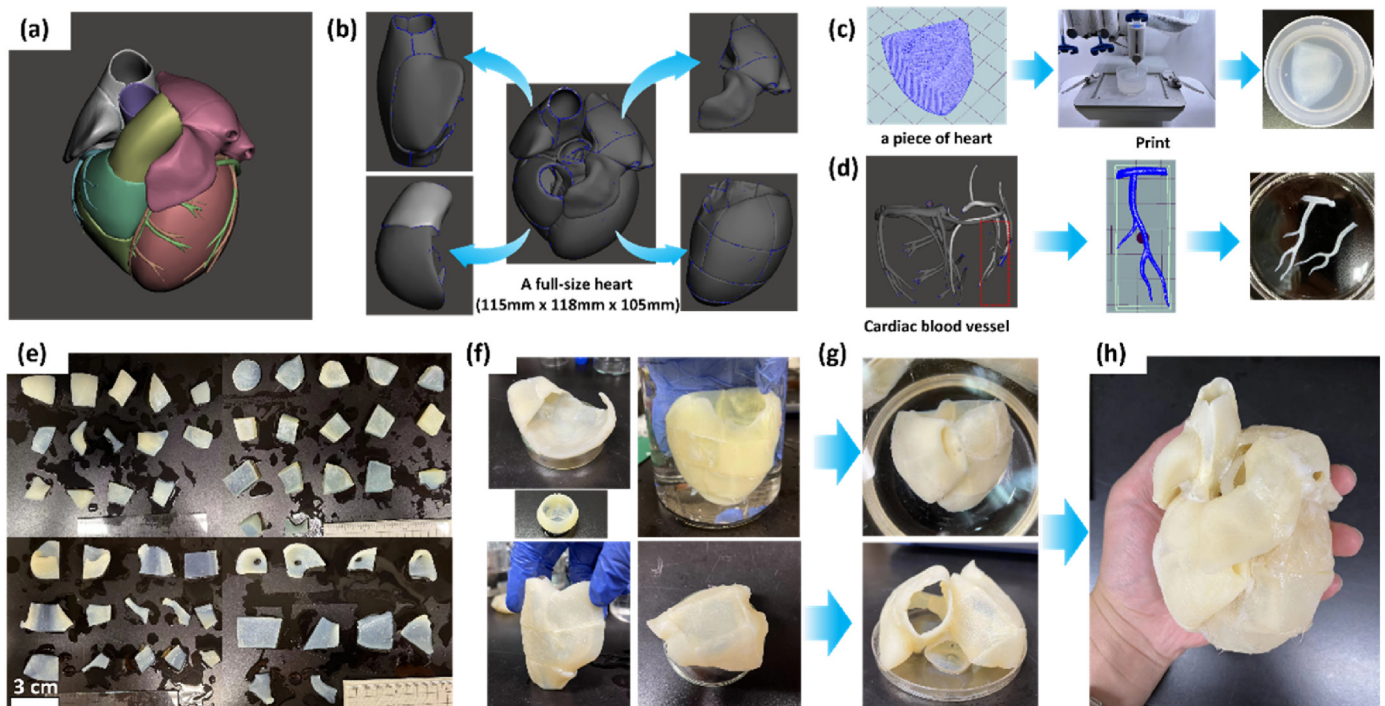
Fig. 4. Construction of a full-size collagen heart by 3D puzzle-inspired assembly of 3D printed blocks. **(a)** A 3D model of a full-size human heart. **(b)** Schematic diagram of the separation of the whole heart into different parts. **(c)** 3D printing process of small pieces of the heart. **(d)** 3D printing process of a segment of the blood vessels on heart. **(e)** Digital photos of the printed small pieces for a full-size heart construction. More than 60 pieces were printed. (**f** and **g**) The assembled process of different parts of the heart. **(h)** The assembled collagen product of a full-size human heart.

accessible strategy for investigation of the interaction between cells.

In tissue engineering, the mechanical property of the substrate is also an important factor that dictates the behavior of the cells growing on it. The 3D puzzle-inspired strategy enables us to assemble biomaterials with different properties, which can benefit investigation into the effect of substrates on cell behavior. To demonstrate this, collagen sheets with different strengths were 3D printed by changing the ink concentration. It was clearly seen that the collagen sheets printed from different ink concentrations differed markedly in strength (Fig. 5 (e)). As shown in Fig. 5 (f) and Fig. S8, the modulus of the collagen sheet increased from 8 kPa of the sample from 0.5 wt% to over 50 kPa of that from 2 wt%. The collagen sheets with various modulus were connected as illustrated in Fig. 5 (g). Our strategy can thus be applied to investigate the effect of the modulus on the cell dispersion. Specifically, the GFP-HUVEC was homogeneously seeded on the assembled collagen substrate and the cell distribution on the substrate was observed during the culture. As a result, the region with a higher modulus exhibited a higher cell density than that with a low modulus. With longer culture time, this trend became more evident, indicating that HUVEC seems likely to migrate to the area with a high modulus substrate (Fig. 5 (h-j)). This result is consistent with the findings of a previous publication [44], where it was concluded that the substrate with a higher modulus may benefit the cell attachment and spreading on it.

It should be noted that the current 3D puzzle-inspired 3D bioprinting strategy is still confronted with some shortcomings: 1. The assembly process is conducted manually and thus it is time-consuming, especially for the large biostructures such as the full-size heart model. 2. The building blocks used in this work were mainly printed from collagen ink. The current printing conditions may not be suitable for other biomaterials. 3. Some tissues with weak mechanical properties may be broken in the connection process. 4. Although the assembly experiments of the cell-loaded blocks were demonstrated, the cells were just loaded on the surface of the printed block. The porous blocks that encapsulate cells inside block may be closer to the actual situation of the real organs,

which will be studied in our future experiments. Despite these limitations, this work demonstrated the great potential of the developed strategy in tissue engineering, opening an alternative path for preparing biostructures with multiple materials, large size and complex geometry for tissue engineering applications.

3. Conclusion

In summary, this work combined the 3D puzzle concept with 3D printing technology to realize the construction of complex tissues or large organ models on a commercial 3D printer. By using the 3D puzzle-inspired strategy, we made a breakthrough in the preparation of a biostructure by assembling the 3D printed "small and simple" bio-blocks into a "large and complex" bioproduct. As demonstrated, complex structures including a picture puzzle consisting of different materials and colors, a collagen "soccer" with a hollow yet closed structure, and even a full-size heart model were successfully produced from the small blocks that were printed separately. These 3D structures were generally difficult to produce by conventional 3D printer. The 3D puzzle-inspired strategy also enables the practical combination of various cells in a specified order, which is conducive to the investigation of the interaction between different kinds of cells. The developed strategy removes the limitation of conventional 3D printing and allows us to prepare organ structures with multiple materials, large size and complex geometry by a versatile and easy-to-operate method, providing an alternative path to the construction of 3D bioproducts for tissue engineering and biomedical application.

4. Experimental section

4.1. Materials

Gellan gum (GG) powder (KELCOGAEL, deacetylated, from SANSHO Co., Ltd) was used as bath material. The collagen powder (Type I, pepsin-solubilized from porcine skin, PSC-1-200-500PW) was provided by Nippi
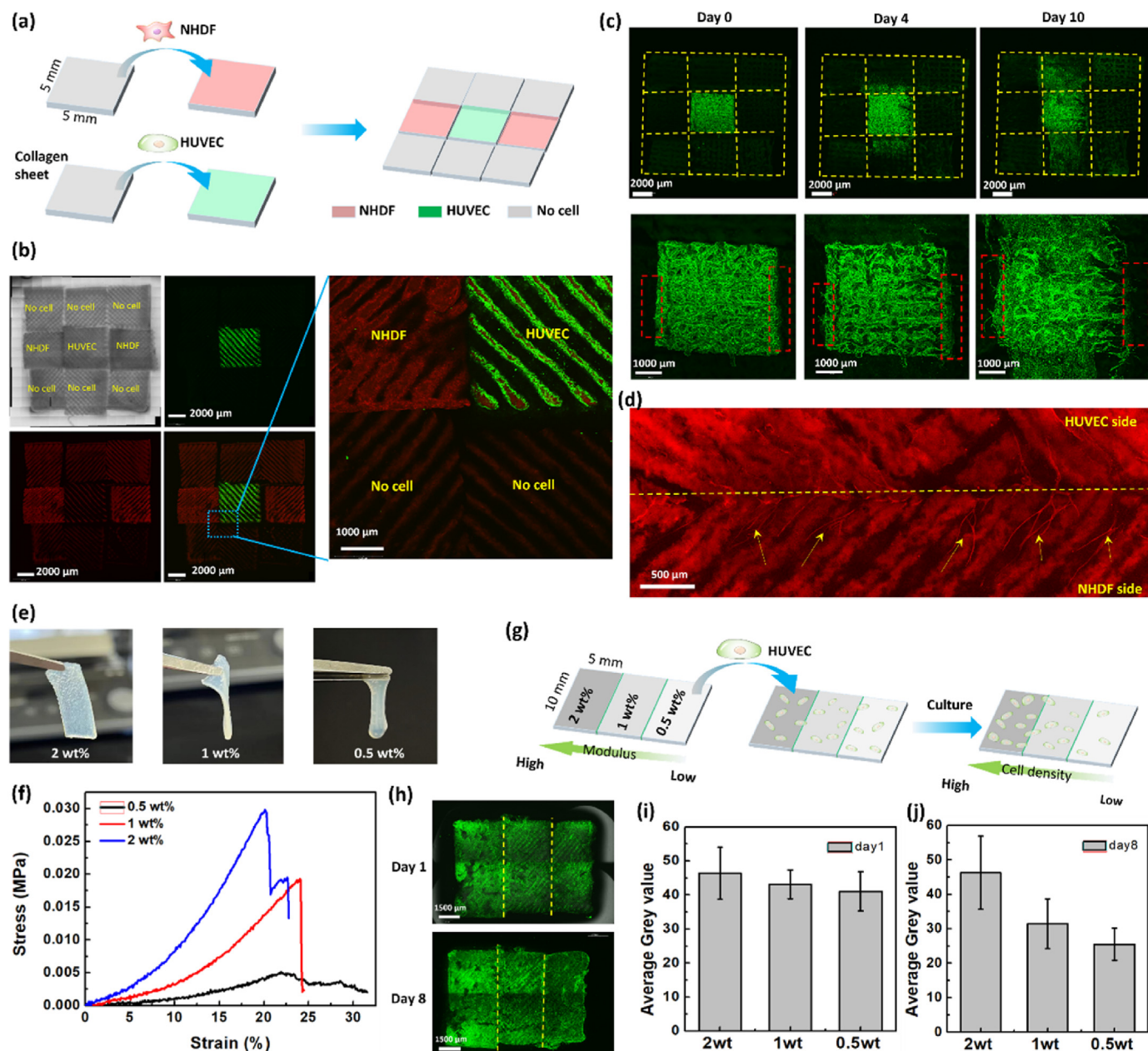
Fig. 5. 3D puzzle-inspired assembly of blocks with various cells fascinate the investigation of the effect of cell location and scaffold modulus on the cell behaviors. **(a)** Scheme of seeding NHDF and HUVEC on the printed collagen square respectively, and the assembled pattern. **(b)** Fluorescence images of the assembled pattern with different cell or no cells. Red indicates the cell tracker-labeled NHDF. Green indicated the location of GFP-HUVEC. **(c)** Fluorescence images of the assembled pieces and the magnified images of the center area, after culture for 0, 4 and 10 days. Green color indicates the GFP-HUVEC. The bottom images are the magnification of the center region in upper images. **(d)** Magnified fluorescence image of the joint region, suggesting the capillary formation at the boundary area. **(e)** Digital photos of the pieces printed from 2, 1 and 0.5 wt% collagen ink. **(f)** Stress-strain curve of the pieces with different collagen concentrations **(g)** Scheme of the assembly of the collagen pieces with different modulus, and then seeding the GFP-HUVEC on the assembled piece to culture for observation. **(h)** are the fluorescence images of the assembled pieces after culture for 1 day and 8 days respectively. **(i)** and **(j)** indicate the average fluorescence intensity at different areas at day 1 and day 8 respectively (measured by Image J).

Co., Ltd, Japan. Trisodium citrate (TSC, 2-hydrated) and Glutaraldehyde (GA, 50% aq.) was purchased from KISHIDA CHEMICAL Co., Ltd. Fibrinogen (F8630) and thrombin (T4648) were purchased from Sigma-Aldrich (MO, USA). Trypsin (209-19182) was obtained from FUJIFILM Wako, Japan. Fluorescein 5-Isothiocyanate (isomer I) (FITC, 16151-66, ≥90.0%(HPLC)) is provided by Nacalai, Co., Ltd. Dulbecco's phosphate buffered saline (PBS) solution was prepared by dissolving the PBS powder (Sigma-Aldrich) in water with the concentration of 9.6 mg/L (for PBS 1×) or 96 mg/L (for PBS 10×), respectively. Oxidized methacrylated alginate (OMA) with 0.85% oxidation and 10.61% methacrylation

degree was friendly provided from university of Illinois Chicago, USA. The synthesis details can be found in the previous publication [45]. Human umbilical vein endothelial cell (HUVEC, C2517A) and Normal human dermal fibroblast (NHDF) cell are purchased from LONZA (Basel, Switzerland). GFP expressed human umbilical vein endothelial cells (GFP-HUVECs) was obtained from Angio-Proteomie (Massachusetts, USA). Dulbecco's modified Eagle medium (DMEM, 08458–16, Nacalai tesque, Kyoto, Japan), KBM VEC-1 basal medium (16030110, Kohjin Bio Co. Ltd., Saitama, Japan), Fetal bovine serum (FBS, 35010CV, Corning, NY, USA), antibiotics (50 U/mL penicillin and 50 μg/mL streptomycin,

Thermo Fisher Scientific, Whaltam, MA, USA) were used in cell culture experiments. 4%-paraformaldehyde (163-20145, FUJIFILM Wako Pure Chemical Corporation), Triton X-100 (T8787, Sigma-Aldrich), Bovine serum albumin (BSA, A3294, Sigma-Aldrich), Anti-CD31 antibody (M0823, Dako, Glostrup, Denmark), Rabbit-Anti-vimentin (monoclonal, ab92547, Abcom), Alexa Fluor 647 (anti-mouse, A21235, Invitrogen, USA) and Hoechst 33342 (H3570, Thermo Fisher, Scientific, Waltham, USA) were used for the fixation and immunostaining experiments. Cell-Tracker™ Deep Red (C34565, Thermofisher, Mw: 698) was the fluorescent labeling for staining of NHDF. Other solvents including ethanol, Dimethyl sulfoxide (DMSO) were chemical pure, and all reagents were used as received.

4.2. Preparation of supporting bath

The GG granular gels were used as the bath for the embedding 3D printing. The preparation of GG bath is as follows. The GG powder was firstly dissolved in PBS at 100 °C with the concentration of 5 mg/mL, and then the solution was cool down to room temperature and kept for at least 3 h to form GG bulk gel. The obtained GG bulk gel was further crashed by a handheld rotor–stator homogenizer (IKEA, T10 Basic) at the maximum power for 6 min. The GG microgels tend to aggregate with each other through the hydrogen bond and ionic interaction, which caused the inhomogeneity of the bath and is not conducive to the printing resolution [46]. To prevent the aggregation of GG particles, TSC solution (1 M, aq.) was added into the GG particles with the final TSC concentration of 0.3 M in bath followed by homogenization for 2 min. Before use, the bath was centrifuged at 2000 rpm for 3 min to remove bubbles. For the printing of 2 wt% collagen ink, the ethanol with the final volume ratio of 30% was added by homogenization and then the mixture was treated by centrifugation at 2000 g for 3 min to remove the supernatant.

4.3. Preparation of ink

The collagen ink was prepared based on our published method [7]. Briefly, the collagen powder was homogenized in PBS 10× for 6 min at r. t. Subsequently, the collagen powder was recycled by centrifugation at 10,000 rpm for 5 min, and then redispersed into PBS 1× by homogenization. The obtained solution was kept at 4 °C overnight for dissolving of collagen. The collagen solution with the concentration of 1 wt% or 2 wt% was prepared by changing the collagen dosage. Before use as ink, the collagen solution should be centrifuged (4000 rpm, 3 min) to remove bubbles. For preparation of ink with black color, 0.5 wt% edible black coloring (Kyoritsu-food, Japan) was mixed into the ink. The OMA ink was prepared by dissolving 4 wt% OMA powder in water, with 0.1% photo-initiator
(2-Hydroxy-40-(2-hydroxyethoxy)-2-methylpropiophenone).

4.4. 3D printing process

The 3D printing was conducted on a commercial 3D printer (Bio-X, CELLINK) in laboratory. For the preparation of a "O", "U" picture puzzles, the collagen or OMA sheet with size of 1 cm × 1 cm was used as building blocks. They are 3D printed in a GG granular bath. Briefly, the GG bath was poured into a plastic vail with a diameter with 3 cm. The collagen ink (1 wt%) was loaded in a pneumatic syringe and a 25-gauge needle with a length of 2.5 cm and an inner diameter of 250 μm was used as the nozzle. The driven air pressure was set to 20-30 kPa (the corresponding linear extrusion speed was 0.25–0.4 cm/s). The nozzle movement speed of 25 mm/s and a layer height of 0.1 mm was used. For the printing of OMA sheets, the 4 wt% OMA and 2 wt% collagen solution were mixed with the volumn ratio of 1:1 to be used as ink. All the printing processes were conducted at room temperature. For the preparation of hollow collagen "soccer", the collagen hexagon and pentagon were printed as the building blocks, by using the 1 wt% and 2 wt% collagen ink respectively. When printing with 2 wt% collagen ink, the bath modified with ethanol was used. The driven air pressure was set to 60-80 kPa. Other conditions are similar with that mentioned above.

After printing, the sample was kept at room temperature for 1 h to make sure the complete gelation of collagen in bath. To improve the mechanical property and stability, GA was used to fix the printed collagen sample. The sample was soaked into 0.5 v/v% GA in 50% ethanol/water mixture solution to be *in situ* cured in bath at room temperature overnight. The cured product was retracted from the bath by repeatedly washing with excessive MiliQ water, and then immersing in 50 mM Tris solution (pH = 7.4) to further remove the remained GG.

4.5. Assembly process and disassociation process

To assemble the printed blocks, the fibrinogen (50 mg/mL) and thrombin (20 unit/mL) in PBS was mixed and used as a "bio-glue" immediately to realize the connection between blocks. In detail, the mixed "bio-glue" was added into the seam between two blocks, and then kept at room temperature for 5-10 min. During this process, the fibrinogen will react with thrombin to form fibrin gel, by which two pieces of blocks can be connected. To indagate the influence of fibrinogen concentration on the final connection strength, the "bio-glue" consisting of 20, 50 and 100 mg/mL of fibrinogen with a constant ratio of thrombin (2 units thrombin per 5 mg fibrinogen) were used to connect two pieces of collagen sheets. The tensile experiments with a tensile speed of 10 mm/min was employed to compare the connection strength of the samples connected by different "bio-glue".

The disassociation of the connected blocks was realized by immersing the sample in 0.1% trypsin in PBS solution and incubation at 37 °C for 20 min, by which the cured "bio-glue", i.e., fibrin gel, between the blocks will be digested by trypsin. As a result, the connected blocks can be disassociated. After washing with PBS solution, these blocks can be reused to build 3D structures.

To visualize the "bio-glue" at the joint of two blocks, 10 wt% of fibrinogen in "bio-glue" was replaced by FITC-labeled fibrinogen. FITC-labeled fibrinogen was synthesized according to reference. [47] The joint region was observed by a confocal laser scanning microscope (CLSM, FV3000, Olympus).

4.6. Construction of full-size collagen heart

For the fabrication of a full-size heart model, the 3D model was divided into small pieces and then printed one by one. Specifically, the full-size heart model was downloaded from internet (https://lifesciencedb.jp/bp3d/). The downloaded heart model was divided to small pieces with width less than 5 cm, and modified to remove non-printable defects by Autodesk Meshmixer (https://www.meshmixer.com/). The obtained 3D model of each part was further converted to Gcode format by slicing software Repetier-Host (https://www.repetier.com/). For the printing of each block, the collagen ink (2 wt% in PBS) was loaded in pneumatic syringe with 25 G needle. The granular Gellan gum (GG) gels that mixed with 30% ethanol was used as a supporting bath. The ink was extruded into the supporting bath to form the designed structure through the programmed movement of nozzle in the bath. For the printing parameters, the syringe pressure of 60–80 kPa, the nozzle movement of 25 mm/s, the 60% infill density and the layer height of 0.1 mm were employed in the printing process. After printing, the sample was kept at room temperature for 3 h to make sure the complete gelation of collagen in bath. Subsequently, the printed sample was crosslinked by immersing in a 0.5% glutaraldehyde (GA) solution in 50% ethanol overnight. The crosslinked sample was further washed by excessive MiliQ water and finally stored in 70% ethanol.

The crosslinked collagen pieces were connected by manually adding the "bio-glue" (mixture of 50 mg/mL Fibrinogen and 20 units/mL of Thrombin) at joint. The big parts of the heart including the left chamber, right chamber, left corona, right corona and other parts were constructed by assembly of the printed small pieces (total more than 60 pieces). Then

further assemble these parts to get the final full-size collagen heart. To realize the correct assembly, before printing we divided the blocks into several categories based on their locations, and every block in each category was numbered in sequence. The blocks were printed and stored according to the numbered sequence. In the assembly process, we used a layer-by-layer connection strategy to assemble these blocks up. Specifically, the blocks belonging to the category that located at the bottom were first connected according to the sequence number. Subsequently, the blocks in the category at the upper location were connected. By this strategy, different parts of the heart including the left atrium, right atrium, left ventricle, and right ventricle were separately constructed. Finally, all parts were assembled to obtain the whole structure of the full-size heart. Because the blocks are designed to have flat edges and the size that match adjacent parts, we can connect the edges of different blocks with a relatively neat alignment. After assembly, the obtained collagen heart model was stored in 70% ethanol aq. to prevent the bacteria.

4.7. Assembly of collagen sheets bearing different cells

The building block strategy can be used to investigate the interaction between different cells. Here the HUVEC cells and NHDF cells were separately cultured on the collagen sheets and then the collagen sheets that bears different cells were connected using the 3D puzzle-inspired method according to a designed pattern. By observing the cell behavior after assembly, the interaction between two kinds of cells can be revealed. In detail, the preparation method is as follows:

1. 3D printing of the collagen sheets. The collagen sheets were used as cell scaffold in the experiments. Collagen sheets (20 mm × 10 mm x 1 mm) was 3D printed on a Bio-X printer by an embedding printing method using the granular gellan gum (GG) gels that mixed with 0.3 M TSC as a supporting bath. The 1 wt% collagen ink was extruded into the supporting bath to form the designed structure through the programmed movement of nozzle in the bath. For the printing parameters, the syringe pressure of 20–30 kPa, the nozzle movement of 25 mm/s, the 99% infill density and the layer height of 0.1 mm were employed in the printing process. The printed sample was crosslinked by 0.25% glutaraldehyde (GA) solution in 50% ethanol overnight. It should be noted that GA is cytotoxic. Therefore, the crosslinked sample was repeatedly washed with excess water to remove the remaining GA.

2. Seed NHDF and HUVEC on the printed collagen sheets. The cross-linked collagen sample was sterilized by immersing in 70% ethanol solution for at least 30 min. Before use as scaffold, the ethanol solution was exchange to PBS by repeatedly wash with PBS for 5 times in a clean bench. The collagen sheets were cut into small pieces with size of 5 mm × 5 mm and put in the bottom of a 24-well plates to be used as scaffold. Then the HUVEC or NHDF cells were seeded on the collagen pieces with a cell density around $1 \times 10^6/cm^2$. Specifically, the HUVEC or NHDF cells were dispersed in medium (KBM for HUVEC and DMEM for NHDF) and then manually added onto the collagen sheets. Then the samples were cultured at 37 °C, 5% CO_2 for 1 day.

3. Connection of the collagen sheets that bears NHDF, HUVEC or no cells together by bio-glue. The collagen sheets bearing different cells were put together according to the patterns as shown as below. The "bio-glue" was added into the joint between the pieces to connect the pieces by the gelation of bio-glue. The assembled samples were put into a 6-well plate. 5 mL of the mixed medium of KBM and DMEM (1:1) was added into the plate and the sample was cultured at 37 °C, 5% CO_2. After culture for 10 days, the sample was fixed by 4% PFA and treat by immunofluorescence staining of the CD31 and nucleus for the observation of the distribution of cells on the assembled sample by CLSM. For the observation of the cell distribution in alive state during the culture process, the GFP-HUVEC and cellTracker-Deep red-treated NHDF were used.

4.8. Characterizations of the printed samples

The mechanical properties were tested by tensile experiments on EZ test (SHIMADZU, EZ/CE) with a sensor of 500 N. The tensile speed was set to 10 mm/min. The morphologies of the connected collagen sheets were observed by a scanning electron microscope (SEM, JSM-7601F, JEOL, Ltd. Tokyo, Japan) at 10 kV. The sample was freeze dried and coated with a thin layer of Osmium by using an ion sputter apparatus to be tested.

CRediT authorship contribution statement

Zheng-Tian Xie: Investigation, Writing – original draft, Writing – review & editing. **Jinfeng Zeng:** Investigation, Writing – original draft, Writing – review & editing. **Shigeru Miyagawa:** Writing – review & editing. **Yoshiki Sawa:** Writing – review & editing. **Michiya Matsusaki:** Supervision, Writing – review & editing, Funding acquisition.

Declaration of competing interest

The authors declare that they have no known competing financial interests or personal relationships that could have appeared to influence the work reported in this paper.

Data availability

Data will be made available on request.

Appendix A. Supplementary data

Supplementary data to this article can be found online at https://doi.org/10.1016/j.mtbio.2023.100726.

References

[1] T. Agarwal, D. Banerjee, R. Konwarh, T. Esworthy, J. Kumari, V. Onesto, P. Das, B.H. Lee, F. Wagener, P. Makvandi, V. Mattoli, S.K. Ghosh, T.K. Maiti, L.G. Zhang, I.T. Ozbolat, Recent advances in bioprinting technologies for engineering hepatic tissue, Mater Sci Eng C Mater Biol Appl 123 (2021) 112013.

[2] Z. Gu, J. Fu, H. Lin, Y. He, Development of 3D bioprinting: from printing methods to biomedical applications, Asian J. Pharm. Sci. 15 (5) (2020) 529–557.

[3] S. Chen, W.S. Tan, M.A. Bin Juhari, Q. Shi, X.S. Cheng, W.L. Chan, J. Song, Freeform 3D printing of soft matters: recent advances in technology for biomedical engineering, Biomed Eng Lett 10 (4) (2020) 453–479.

[4] D. Ahn, L.M. Stevens, K. Zhou, Z.A. Page, Rapid high-resolution visible light 3D printing, ACS Cent. Sci. 6 (9) (2020) 1555–1563.

[5] T.J. Hinton, Q. Jallerat, R.N. Palchesko, J.H. Park, M.S. Grodzicki, H.J. Shue, M.H. Ramadan, A.R. Hudson, A.W. Feinberg, Three-dimensional printing of complex biological structures by freeform reversible embedding of suspended hydrogels, Sci. Adv. 1 (9) (2015) e1500758.

[6] Z.T. Xie, D.H. Kang, M. Matsusaki, Resolution of 3D bioprinting inside bulk gel and granular gel baths, Soft Matter 17 (39) (2021) 8769–8785.

[7] D.H. Kang, F. Louis, H. Liu, H. Shimoda, Y. Nishiyama, H. Nozawa, M. Kakitani, D. Takagi, D. Kasa, E. Nagamori, S. Irie, S. Kitano, M. Matsusaki, Engineered whole cut meat-like tissue by the assembly of cell fibers using tendon-gel integrated bioprinting, Nat. Commun. 12 (1) (2021) 5059.

[8] A.C. Daly, M.D. Davidson, J.A. Burdick, 3D bioprinting of high cell-density heterogeneous tissue models through spheroid fusion within self-healing hydrogels, Nat. Commun. 12 (1) (2021) 753.

[9] W. Sun, B. Starly, A.C. Daly, J.A. Burdick, J. Groll, G. Skeldon, W. Shu, Y. Sakai, M. Shinohara, M. Nishikawa, J. Jang, D.W. Cho, M. Nie, S. Takeuchi, S. Ostrovidov, A. Khademhosseini, R.D. Kamm, V. Mironov, L. Moroni, I.T. Ozbolat, The bioprinting roadmap, Biofabrication 12 (2) (2020) 022002.

[10] A. Shapira, N. Noor, H. Oved, T. Dvir, Transparent support media for high resolution 3D printing of volumetric cell-containing ECM structures, Biomed. Mater. 15 (4) (2020) 045018.

[11] L. Ning, R. Mehta, C. Cao, A. Theus, M. Tomov, N. Zhu, E.R. Weeks, H. Bauser-Heaton, V. Serpooshan, Embedded 3D bioprinting of gelatin methacryloyl-based constructs with highly tunable structural fidelity, ACS Appl. Mater. Interfaces 12 (40) (2020) 44563–44577.

[12] A. McCormack, C.B. Highley, N.R. Leslie, F.P.W. Melchels, 3D printing in suspension baths: keeping the promises of bioprinting afloat, Trends Biotechnol. 38 (6) (2020) 584–593.

[13] Y.J. Choi, Y.J. Jun, D.Y. Kim, H.G. Yi, S.H. Chae, J. Kang, J. Lee, G. Gao, J.S. Kong, J. Jang, W.K. Chung, J.W. Rhie, D.W. Cho, A 3D cell printed muscle construct with tissue-derived bioink for the treatment of volumetric muscle loss, Biomaterials 206 (2019) 160–169.

[14] M.A. Heinrich, R. Bansal, T. Lammers, Y.S. Zhang, R. Michel Schiffelers, J. Prakash, 3D-Bioprinted mini-brain: a glioblastoma model to study cellular interactions and therapeutics, Adv. Mater. 31 (14) (2019) e1806590.

[15] Y.N. Kang, P. Datta, S. Shanmughapriya, I.T. Ozbolat, 3D bioprinting of tumor models for cancer research, ACS Appl. Bio Mater. 3 (9) (2020) 5552–5573.

[16] D.B. Kolesky, R.L. Truby, A.S. Gladman, T.A. Busbee, K.A. Homan, J.A. Lewis, 3D bioprinting of vascularized, heterogeneous cell-laden tissue constructs, Adv. Mater. 26 (19) (2014) 3124–3130.

[17] W. Wu, A. DeConinck, J.A. Lewis, Omnidirectional printing of 3D microvascular networks, Adv. Mater. 23 (24) (2011) H178–H183.

[18] S.G. Patricio, L.R. Sousa, T.R. Correia, V.M. Gaspar, L.S. Pires, J.L. Luis, J.M. Oliveira, J.F. Mano, Freeform 3D printing using a continuous viscoelastic supporting matrix, Biofabrication 12 (3) (2020) 035017.

[19] M.A. Skylar-Scott, S.G.M. Uzel, L.L. Nam, J.H. Ahrens, R.L. Truby, S. Damaraju, J.A. Lewis, Biomanufacturing of organ-specific tissues with high cellular density and embedded vascular channels, Sci. Adv. 5 (9) (2019) eaaw2459.

[20] Y. Wu, P. Kennedy, N. Bonazza, Y. Yu, A. Dhawan, I. Ozbolat, Three-Dimensional bioprinting of articular cartilage: a systematic review, Cartilage 12 (1) (2021) 76–92.

[21] B.A.G. Melo, Y.A. Jodat, S. Mehrotra, M.A. Calabrese, T. Kamperman, B.B. Mandal, M.H.A. Santana, E. Alsberg, J. Leijten, S.R. Shin, 3D printed cartilage-like tissue constructs with spatially controlled mechanical properties, Adv. Funct. Mater. 29 (51) (2019).

[22] O. Jeon, Y.B. Lee, H. Jeong, S.J. Lee, D. Wells, E. Alsberg, Individual cell-only bioink and photocurable supporting medium for 3D printing and generation of engineered tissues with complex geometries, Mater. Horiz. 6 (8) (2019) 1625–1631.

[23] A. Lee, A.R. Hudson, D.J. Shiwarski, J.W. Tashman, T.J. Hinton, S. Yerneni, J.M. Bliley, P.G. Campbell, A.W. Feinberg, 3D bioprinting of collagen to rebuild components of the human heart, Science 365 (6452) (2019) 482–487.

[24] M.E. Prendergast, J.A. Burdick, Recent advances in enabling technologies in 3D printing for precision medicine, Adv. Mater. 32 (13) (2020) e1902516.

[25] K. Karzynski, K. Kosowska, F. Ambrozkiewicz, A. Berman, J. Cichon, M. Klak, M. Serwanska-Swietek, M. Wszola, Use of 3D bioprinting in biomedical engineering for clinical application, Med. Stud. Studia Medyczne 34 (1) (2018) 93–97.

[26] W. Peng, P. Datta, B. Ayan, V. Ozbolat, D. Sosnoski, I.T. Ozbolat, 3D bioprinting for drug discovery and development in pharmaceutics, Acta Biomater. 57 (2017) 26–46.

[27] I.T. Ozbolat, Bioprinting scale-up tissue and organ constructs for transplantation, Trends Biotechnol. 33 (7) (2015) 395–400.

[28] A. Shapira, T. Dvir, 3D tissue and organ printing-hope and reality, Adv. Sci. (Weinh) 8 (10) (2021) 2003751.

[29] A.W. Feinberg, J.S. Miller, Progress in three-dimensional bioprinting, MRS Bull. 42 (8) (2017) 557–562.

[30] M.A. Skylar-Scott, J. Mueller, C.W. Visser, J.A. Lewis, Voxelated soft matter via multimaterial multinozzle 3D printing, Nature 575 (7782) (2019) 330–335.

[31] T.J. Hinton, A. Lee, A.W. Feinberg, 3D bioprinting from the micrometer to millimeter length scales: size does matter, Curr. Opin. Biomed. Eng. 1 (2017) 31–37.

[32] E. Mirdamadi, J.W. Tashman, D.J. Shiwarski, R.N. Palchesko, A.W. Feinberg, FRESH 3D bioprinting a full-size model of the human heart, ACS Biomater. Sci. Eng. 6 (11) (2020) 6453–6459.

[33] C.D. Morley, S.T. Ellison, T. Bhattacharjee, C.S. O'Bryan, Y. Zhang, K.F. Smith, C.P. Kabb, M. Sebastian, G.L. Moore, K.D. Schulze, S. Niemi, W.G. Sawyer, D.D. Tran, D.A. Mitchell, B.S. Sumerlin, C.T. Flores, T.E. Angelini, Quantitative characterization of 3D bioprinted structural elements under cell generated forces, Nat. Commun. 10 (1) (2019) 3029.

[34] A.M. Compaan, K. Song, W. Chai, Y. Huang, Cross-linkable microgel composite matrix bath for embedded bioprinting of perfusable tissue constructs and sculpting of solid objects, ACS Appl. Mater. Interfaces 12 (7) (2020) 7855–7868.

[35] N. Noor, A. Shapira, R. Edri, I. Gal, L. Wertheim, T. Dvir, 3D printing of personalized thick and perfusable cardiac patches and hearts, Adv. Sci. (Weinh) 6 (11) (2019) 1900344.

[36] Q. Gao, Z. Liu, Z. Lin, J. Qiu, Y. Liu, A. Liu, Y. Wang, M. Xiang, B. Chen, J. Fu, Y. He, 3D bioprinting of vessel-like structures with multilevel fluidic channels, ACS Biomater. Sci. Eng. 3 (3) (2017) 399–408.

[37] Y. Jo, D.G. Hwang, M. Kim, U. Yong, J. Jang, Bioprinting-assisted tissue assembly to generate organ substitutes at scale, Trends Biotechnol. 41 (1) (2023) 93–105.

[38] R. Subbiah, C. Hipfinger, A. Tahayeri, A. Athirasala, S. Horsophonphong, G. Thrivikraman, C.M. Franca, D.A. Cunha, A. Mansoorifar, A. Zahariev, J.M. Jones, P.G. Coelho, L. Witek, H. Xie, R.E. Guldberg, L.E. Bertassoni, 3D printing of microgel-loaded modular microcages as instructive scaffolds for tissue engineering, Adv. Mater. 32 (36) (2020) e2001736.

[39] C.F. Guimarães, L. Gasperini, A.P. Marques, R.L. Reis, The stiffness of living tissues and its implications for tissue engineering, Nat. Rev. Mater. 5 (5) (2020) 351–370.

[40] A. du Plessis, A.J. Babafemi, S.C. Paul, B. Panda, J.P. Tran, C. Broeckhoven, Biomimicry for 3D concrete printing: a review and perspective, Addit. Manuf. 38 (2021).

[41] A. Jafari, Z. Ajji, A. Mousavi, S. Naghieh, S.A. Bencherif, H. Savoji, Latest advances in 3D bioprinting of cardiac tissues, Adv. Mater. Technol. 7 (11) (2022).

[42] S. Chae, D.W. Cho, Biomaterial-based 3D bioprinting strategy for orthopedic tissue engineering, Acta Biomater. 156 (2022) 4–20, https://doi.org/10.1016/j.actbio.2022.08.004.

[43] H. Wang, H. Yu, X. Zhou, J. Zhang, H. Zhou, H. Hao, L. Ding, H. Li, Y. Gu, J. Ma, J. Qiu, D. Ma, An overview of extracellular matrix-based bioinks for 3D bioprinting, Front. Bioeng. Biotechnol. 10 (2022) 905438.

[44] M.C. Lampi, M. Guvendiren, J.A. Burdick, C.A. Reinhart-King, Photopatterned hydrogels to investigate the endothelial cell response to matrix stiffness heterogeneity, ACS Biomater. Sci. Eng. 3 (11) (2017) 3007–3016.

[45] O. Jeon, D.S. Alt, S.M. Ahmed, E. Alsberg, The effect of oxidation on the degradation of photocrosslinkable alginate hydrogels, Biomaterials 33 (13) (2012) 3503–3514.

[46] Z.T. Xie, J. Zeng, D.H. Kang, S. Saito, S. Miyagawa, Y. Sawa, M. Matsusaki, 3D printing of collagen scaffold with enhanced resolution in a citrate-modulated gellan gum microgel bath, Adv Healthc Mater (2023) e2301090.

[47] T. Quach, M. Tippens, F. Szlam, R. Van Dyke, J.H. Levy, M. Csete, Quantitative assessment of fibrinogen cross-linking by epsilon aminocaproic acid in patients with end-stage liver disease, Liver Transplant. 10 (1) (2004) 123–128.